Prace Naukowe Instytutu Maszyn, Napędów i Pomiarów Elektrycznych
Nr 70 Politechniki Wrocławskiej Nr 70

Studia i Materiały Nr 34 2014

induction motor, synchronous rotating frame,
vector control, mathematical model

Bronislav FIRAGO*, Dmitry VASILYEV*

CONCERNING THE VECTOR CONTROL OF A SQUIRREL-CAGE INDUCTION MOTOR

A technique for investigation of electric drive dynamics when an induction motor operates at the direct vector control with alignment of the axis x of synchronous rotating frame x–y along the rotor flux linkage vector is presented here. Simulation results of the specific electric drive verify the faithfulness of recommended technique.

1. INTRODUCTION

The purpose of squirrel-cage induction motor vector control is to obtain such conditions that exist in a separately excited direct current motor (SE DCM): 1) orthogonality of vectors which form the motor electromagnetic torque, 2) the possibility to control the magnetic flux linkage and electromagnetic torque independently. In order to gain the independent control of flux linkage and electromagnetic torque in the squirrel-cage induction motor which has only one control channel for the stator voltage (or current), it is necessary to insert the compensating voltages in a control system of "frequency converter–induction motor" (FC–IM). This action permits us to distinguish between two components of the stator current vector: a "field component" that determines the flux linkage and a "torque component" that determines the motor electromagnetic torque [1, 2]. These components of the induction motor stator current vector are akin to the excitation current and the armature current of the SE DCM accordingly.

At the present time no less than 20 types of the electric motor vector control can be counted [3]. Out of this variety the following types of vector control are used mostly:

* Belarusian National Technical University, Belarus, 220013, Minsk, Nezavisimosti av., 65, e-mail: dmy@tut.by

1) direct vector control with the flux linkage estimation and velocity sensor,
2) direct sensorless vector control where the flux linkage and motor velocity are calculated via the dynamic model block diagrams,
3) indirect vector control with a velocity sensor,
4) indirect sensorless vector control.

The most simple and widespread type of vector control is the indirect sensorless vector control of an induction motor. The drawback of this type of vector control consists in the dependence of accuracy of its realization on accuracy of induction motor parameter identification because the motor parameters vary according to temperature, frequency, value of current and magnetic saturation.

Because of inaccurate motor parameter identification and dependence of parameters on induction motor operating conditions the properties of induction motor at the indirect sensorless vector control differ essentially from the specified ones. For the purpose of improvement of indirect sensorless vector control indices, the special algorithms for motor parameter identification on the basis of rated data are introduced and then the autotuning of parameters is used during motor operation.

Nevertheless, the indirect sensorless vector control systems don't permit to control the induction motor electromagnetic torque at zero velocity. In this connection, for hoisting electric drives, where it is needed to control the electromagnetic torque at zero motor velocity, the vector control systems are developed with inclusion of velocity sensors.

From the above mentioned four vector control types the direct and indirect vector control with alignment of the axis x of synchronous rotating frame x-y along the rotor flux linkage vector are mostly used as in these cases simpler relationships exist between regulated values. Although these two vector control types are rather well represented in the technical publications [4–7], there are some issues that need refinements and deserve further consideration. These issues include: the faithful representation of dynamic model block diagrams in correspondence with the modern vector control realization, revision of analytical expressions for regulator parameter determination as in some publications, for example [5], there are uncertainties and inaccuracies in given formulae.

2. MATHEMATICAL MODEL AND DYNAMIC MODEL BLOCK DIAGRAM OF THE EQUIVALENT TWO-PHASE INDUCTION MOTOR IN A SYNCHRONOUS ROTATING FRAME

The mathematical model of the equivalent two-phase induction motor for electric and magnetic components in a synchronous rotating frame x-y has been obtained in [2]:

$$\left.\begin{aligned}
u_{1x} &= i_{1x}R_1 + \frac{d\Psi_{1x}}{dt} - \omega_1\Psi_{1y} \\
u_{1y} &= i_{1y}R_1 + \frac{d\Psi_{1y}}{dt} - \omega_1\Psi_{1x} \\
0 &= i'_{2x}R'_2 + \frac{d\Psi_{2x}}{dt} - (\omega_1 - \omega_{el})\Psi_{2y} \\
0 &= i'_{2y}R'_2 + \frac{d\Psi_{2y}}{dt} + (\omega_1 - \omega_{el})\Psi_{2x} \\
\Psi_{1x} &= L_1 i_{1x} + L_{12} i'_{2x} \\
\Psi_{1y} &= L_1 i_{1y} + L_{12} i'_{2y} \\
\Psi_{2x} &= L_2 i'_{1x} + L_{12} i_{1x} \\
\Psi_{2y} &= L_2 i'_{2y} + L_{12} i_{1y} \\
M &= \frac{3}{2} p_{pol} L_{12} (i_{1y} i'_{2x} - i_{1x} i'_{2y})
\end{aligned}\right\}, \tag{1}$$

where

$$\left.\begin{aligned}
L_1 &= L_{12} + L_{1\sigma} \\
L_2 &= L_{12} + L_{2\sigma}
\end{aligned}\right\}, \tag{2}$$

$L_{12} = L_\mu$ – maximal magnitude of mutual inductance for a three-phase induction motor,
$L_{1\sigma}, L_{2\sigma}$ – leakage inductances of stator and rotor,
R_1, R_2 – resistances of the stator and rotor (reduced) windings,
u_{1x}, u_{1y} – stator voltage components of induction motor in the axes *x*-*y*,
i_{1x}, i_{1y} – stator current components of induction motor in the axes *x*-*y*,
Ψ_{1x}, Ψ_{1y} – stator flux linkage components of induction motor in the axes *x*-*y*,
Ψ_{2x}, Ψ_{2y} – rotor flux linkage components of induction motor in the axes *x*-*y*,
i'_{2x}, i'_{2y} – reduced rotor current components of induction motor in the axes *x*-*y*,
M – induction motor electromagnetic torque,
p_{pol} – pairs of pole,
$\omega_{el} = p_{pol}\omega$ – electrical rotor angular velocity,
ω – mechanical rotor angular velocity,
$\omega_1 = 2\pi f_1$ – angular frequency,
f_1 – frequency of the stator voltage.

In alignment of the axis *x* along the rotor flux linkage vector we have the relationships [1]:

$$i'_{2x} = 0, \quad \Psi_{2y} = 0 \tag{3}$$

that permits us to transform the mathematical model (1) to another form:

$$\left.\begin{aligned} u_{1x} &= i_{1x}R_1 L_{1\sigma}\frac{di_{1x}}{dt} - \omega_1 \sigma L_1 i_{1y} \\ u_{1y} &= i_{1y}R_1 + \sigma L_1 \frac{di_{1y}}{dt} + \omega_1(\Psi_{2x} + L_{1\sigma} i_{1x} \\ \Psi_{2x} &+ T_2 \frac{d\Psi_{2x}}{dt} = L_{12} i_{1x} \\ M &= \frac{3}{2} p_{pol} K_r i_{1y} \Psi_{2x} \\ \Delta\omega_{el} &= \omega_1 - \omega_{el} = \frac{1}{T_2}\frac{i_{1y}}{i_{1x}} \end{aligned}\right\}, \tag{4}$$

where

$\sigma = 1 - \dfrac{L_{12}}{L_1 L_2}$ is a leakage coefficient,

$T_2 = \dfrac{L_2}{R_2'}$ is a rotor electromagnetic time constant,

$K_r = \dfrac{L_{12}}{L_2}$ is a coefficient of rotor magnetic coupling.

The mathematical model (4) contains the EMF of rotation:

$$\left.\begin{aligned} e_{1x} &= -\omega_1 \sigma L_1 i_{1y} \\ e_{1y} &= \omega_1(\Psi_{2x} + L_{1\sigma} i_{1x} \end{aligned}\right\} \tag{5}$$

due to rotation of the synchronous frame *x*-*y* relative to a stator stationary frame $\alpha - \beta$.

The angular frequency ω_1 of stator voltage can be derived from (4) on the basis of equality:

$$\omega_1 = \omega_{el} + \Delta\omega_{el} . \tag{6}$$

For independent assignment of currents i_{1x} and i_{1y}, that determine the flux linkage and electromagnetic torque, the compensating voltages:

$$u_{cx} = -e_{1x}, \quad u_{cy} = -e_{1y} \tag{7}$$

are inserted in voltage equations of the mathematical model (4).

With the introduction of such a compensation the stator voltage components become decoupled:

$$\left.\begin{aligned} u_{1x}^{*} &= u_{1x} + u_{cx} = R_1\left(i_{1x} + T_{1x}\frac{di_{1x}}{dt}\right) \\ u_{1y}^{*} &= u_{1y} + u_{cy} = R_1\left(i_{1y} + T_{1y}\frac{di_{1y}}{dt}\right) \end{aligned}\right\}, \tag{8}$$

where

$$T_{1x} = \frac{L_{1\sigma}}{R_1}, \quad T_{1y} = \frac{\sigma L_1}{R_1} \tag{9}$$

are time constants.

Now with a help of voltages u_{1x}^{*}, u_{1y}^{*} one can assign independently "field" i_{1x} and "torque" i_{1y} components of stator current vector $\bar{i}_1$, i.e. the rotor flux linkage and electromagnetic torque for a specified induction motor.

The reference values of $i_{1x,\,ref}$ and $i_{1y,\,ref}$ are calculated as:

$$i_{1x,\,ref} = \frac{\Psi_{2x,\,ref}}{L_{12}}, \tag{10}$$

$$i_{1y,\,ref} = \frac{2M_{ref}}{3p_{pol}K_r\Psi_{2x}} \tag{11}$$

on the assumption that magnitudes of $\Psi_{2x,\,ref}$ and M_{ref} are specified.

Using the mathematical model (4), one can obtain a formula for calculation of the rotor flux linkage amplitude under motor rated conditions:

$$\Psi_{2m.\,rat} = \frac{1}{p_{pol}}\sqrt{\frac{2M_{el.\,rat}R_2'}{3\omega_{0rat}s_{rat}}}, \tag{12}$$

where

$M_{el.\,rat}$ – rated electromagnetic torque of induction motor,

ω_{0rat} – synchronous angular velocity at rated frequency f_{0rat},

s_{rat} – rated slip.

After finding the reference current values $i_{1x,\,ref}$ and $i_{1y,\,ref}$ it is necessary to return to stator voltage equations in the mathematical model (4), where the EMF exist, for determination of reference voltage components:

$$\left.\begin{aligned} u_{1x,\,ref} &= i_{1x,\,ref}R_1 + L_{1\sigma}\frac{di_{1x,\,ref}}{dt} - \omega_1\sigma L_1 i_{1y,\,ref} \\ u_{1y,\,ref} &= i_{1y,\,ref}R_1 + \sigma L_1\frac{di_{1y,\,ref}}{dt} + \omega_1(\Psi_{2x,\,ref} + L_{1\sigma}i_{1x,\,ref}) \end{aligned}\right\}, \tag{13}$$

which are used to calculate the reference voltage first harmonic amplitude:

$$U_{1m,\ rat} = \sqrt{u_{1x,\,ref}^2 + u_{1y,\,ref}^2}\ . \tag{14}$$

Now to the mathematical model (4) we add the equation of electric drive motion

$$M - M_s = J\frac{d\omega}{dt}, \tag{15}$$

where

M_s – static resistive torque of load,

J – electric drive moment of inertia.

Thereafter we construct the dynamic model block diagram of equivalent two-phase induction motor with alignment of the axis x along the rotor flux linkage vector (Fig. 1).

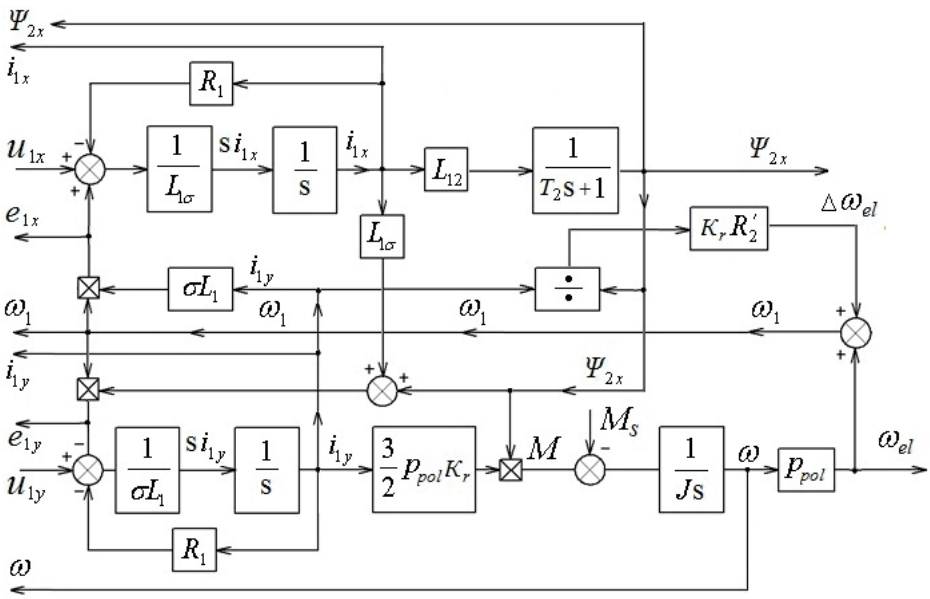

Fig. 1. Dynamic model block diagram of the equivalent two-phase induction motor with alignment of the axis x of synchronous rotating frame x-y along the rotor flux linkage vector

This dynamic model block diagram has an input voltage u_{1x} for the axis x. Output values for the axis x are: the EMF e_{1x}, field current i_{1x} and rotor flux linkage Ψ_{2x}. Accordingly, for the axis y the voltage u_{1y} is an input and the EMF e_{1y}, torque current i_{1y}, rotor angular velocity ω and angular frequency ω_1 are the output values. All values of the dynamic model block diagram are determined by physical parameters of electrical drive at the given vector control. In the direct vector control which we shall consider further a structure of induction motor control incorporates two channels: a flux linkage and an angular velocity (Fig. 2).

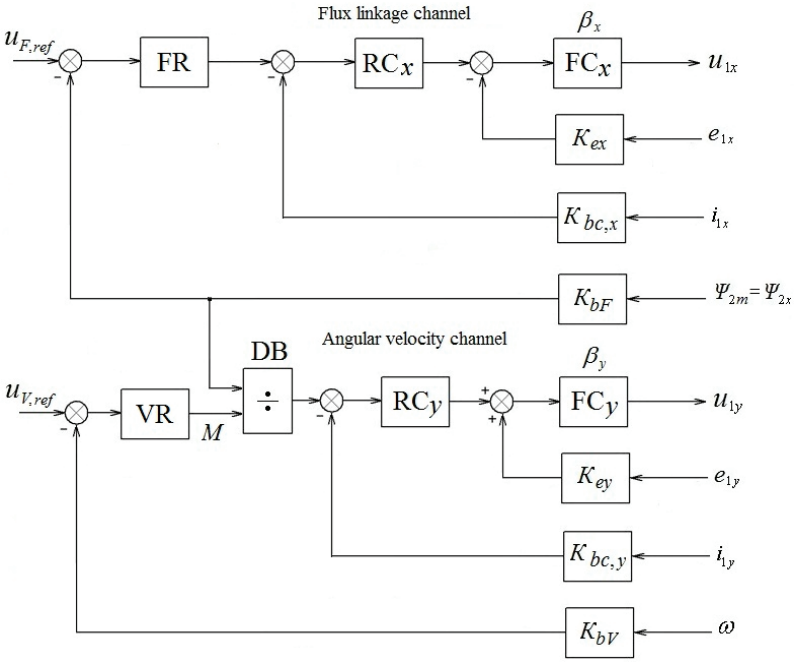

Fig. 2. Block diagram of the induction motor vector control system with alignment of the axis x along the rotor flux linkage vector

The flux linkage channel consists of: a flux linkage regulator FR, a field current regulator RC_x, a frequency converter FC_x with a voltage gain coefficient β_x and a block where the EMF e_{1x} is compensated for the axis x.

The angular velocity channel incorporates: an angular velocity regulator VR, a division block DB for dividing the electromagnetic torque signal by the rotor flux linkage signal, a torque current regulator RC_y and a frequency converter FC_y with a voltage gain coefficient β_y and a block where the EMF e_{1y} is compensated for the axis y.

As usually, in an analogue control system the maximal value of regulator input signal is not in excess of 10 volt. Therefore, to connect a physical object that is represented

here as the dynamic model block diagram of induction motor with a control system, it is necessary to introduce the scale coefficients for each measured value: EMF for the axes *x* and *y*, the field and torque currents, the flux linkage and angular rotor velocity. These scale coefficient values going from a dynamic model block diagram (Fig. 1) to a control system (Fig. 2) are calculated as follows:

$$K_{sc} = \frac{10}{N_{\max}},$$

where $N_{\max}$ is a maximal magnitude of a physical value computed at the output of dynamic model block diagram.

It is clear that scale coefficients K_{sc} can have the dimensions or be dimensionless in dependence on the dimension of measured physical value $N_{\max}$.

The voltage gaining coefficients of frequency converter in the axes *x* and *y* are computed as:

$$\beta_x = \frac{u_{1x,\max}}{10}, \quad \beta_y = \frac{u_{1y,\max}}{10},$$

where $u_{1x,\max}$ and $u_{1y,\max}$ are the maximal voltage magnitudes in the axes *x* and *y* accordingly. As a rule, the equalities are used:

$$u_{1x,\max} = u_{1x,ref}, \quad u_{1y,\max} = u_{1y,ref}.$$

A peculiarity appears when the voltage first harmonic gain coefficients are determined for a frequency converter output. If the phase-to-neutral output voltage of frequency converter is formed under the scalar frequency control via a sinusoidal PWM using DC voltage U_d, the maximal voltage first harmonic amplitude will be equal to

$$U_{1,m} = \frac{U_d}{2}.$$

Then, for the induction motor phase-to-neutral RMS voltage 220 V we have the amplitude $U_{1,m} = \sqrt{2 \cdot 220} = 311\ \text{V}$ that requires a DC source with the voltage

$$U_d = 2 \cdot 311 = 622\ \text{V}.$$

When a frequency converter is supplied by means of a three phase diode bridge rectifier with the input phase-to-phase RMS voltage 400 V, the average value of DC voltage will be equaled to

$$U_d = 1.35 \cdot 400 = 540\ \text{V}$$

that is less than the needed value of 622 V.

To use the rated power of induction motor there appears a need for applying a step up input transformer that is not justified economically. For the same reason the contemporary frequency converters include the space vector pulse-width modulation (SV PWM) which provides the first voltage harmonic amplitude

$$U_{1,m} = \frac{U_d}{\sqrt{3}} = \frac{540}{\sqrt{3}} = 311\,\text{V}$$

at a frequency converter output when the three-phase diode bridge rectifiers are used at the supply voltage of 400 V (RMS). But it should be remembered that an increase of the first voltage harmonic under application of SV PWM is achieved at the cost of higher harmonic increase.

The possibility to use the three-phase diode bridge rectifiers at the input of frequency converters with supply voltage of 400 V RMS relates to the scalar frequency control. For the vector control with rotor flux linkage stabilization a greater voltage value than 540 V for a DC circuit is required.

If to take into account the maximal value of modulation depth equaled to $m = 0.96$, then a DC voltage must be approximately about 580–600 V in order to create the required amplitude of the first voltage harmonic at rated frequency 50 Hz.

These peculiarities have to be taken into consideration during the construction and application of induction motor vector control systems.

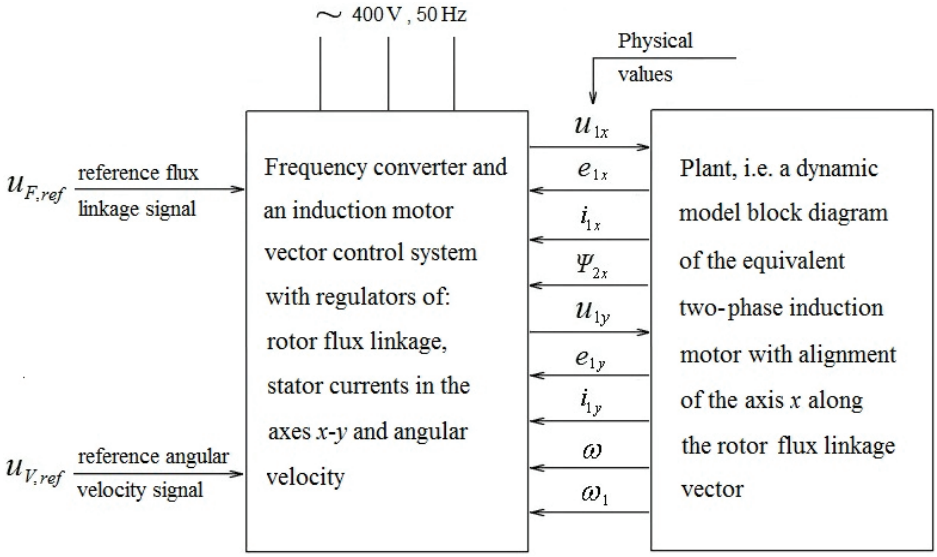

Fig. 3. Generalized structure of the induction motor vector control with alignment of the axis *x* along the rotor flux linkage vector

Usually the induction motor vector control systems include the PI-regulators for the flux linkage, currents and velocity. But a vector control system has coupled channels for the control of the rotor flux linkage and angular velocity because a reference torque (current) signal is a result of dividing the reference torque signal at the angular velocity regulator output by the rotor flux linkage signal (Fig. 2).

On the basis of the described material one can propose a generalized structure for induction motor vector control with alignment of the axis *x* along the rotor flux linkage vector shown in Fig. 3.

Presented in this article technique of induction motor vector control investigation is illustrated with calculation and simulation results.

3. CALCULATION AND SIMULATION RESULTS

The induction motor 4A132S4У3 used for simulation via Matlab has the following rated data:

$$P_{rat} = 7.5 \text{ kW};\ U_{rat} = 380/220 \text{ V};\ f_{1rat} = 50 \text{ Hz};\ s_{rat} = 3\%;\ \eta_{rat} = 87.5\%;$$

$$\cos\varphi_{rat} = 0.86;\ \frac{M_{\max}}{M_{rat}} = 2.2;\ \frac{M_{st}}{M_{rat}} = 2.0;\ p_{pol} = 2;\ J_{m.} = 0.028 \text{ kg}\cdot\text{m}^2.$$

Parameters of the induction motor equivalent circuit:

$$R_1 = 0.70\ \Omega;\ X_1 = 1.23\ \Omega;\ X_\mu = 43.53\ \Omega;\ R_2' = 0.48\ \Omega;\ X_2' = 1.89\ \Omega.$$

Calculated values:

$$L_{1\sigma} = 0.0039 \text{ H};\ L_{2\sigma} = 0.006 \text{ H};\ L_{12} = 0.139 \text{ H};\ L_1 = 0.143 \text{ H};\ L_2 = 0.145 \text{ H};$$

$$\sigma = 0.068;\ K_r = 0.96;\ \Psi_{2m,rat} = 0.9 \text{ Wb};\ I_{1rat} = 15.16 \text{ A};\ M_{rat} = 49 \text{ N}\cdot\text{m};$$

$$M_{ref} = 1.5M_{rat} = 73.5 \text{ N}\cdot\text{m};\ i_{1x,ref} = 6.47 \text{ A};\ i_{1y,ref} = 28.36 \text{ A};$$

$$I_{1m,ref}' \sqrt{i_{1x,ref}^2 + i_{1y,ref}^2} = 29.09 \text{ A};\ u_{1z,ref} = -82.064 \text{ V};$$

$$u_{1y,ref} = 310.34 \text{ V};\ U_{1m,ref} = 321 \text{ V}.$$

It is assumed that $U_d = 600$ V, then

$$m = \frac{\sqrt{3}U_{1m,ref}}{U_d} = 0.925,$$

$$\beta_x = \frac{u_{1x,\,ref}}{10} = 8.2;\ \ \beta_y = \frac{u_{1y,\,ref}}{10} = 31,$$

$$e_{1x,\,ref} = -\omega_{1ref}\sigma L_1 i_{1y,\,ref} = 2\times\pi f_{1ref}\times\sigma L_1 i_{1y,\,ref}$$

$$= -2\times 3.14\times 50\times 0.068\times 0.143\times 28.36 = -86.59,$$

$$e_{1y,\,ref} = -\omega_{1ref}(\Psi_{2x,\,m} + L_{1\sigma} i_{1x,\,ref}) = 3.14\times(0.9 + 0.0039\times 6.47) = 290.52\,V,$$

$$K_{ex} = \frac{10}{86.59} = 0.115;\ \ K_{ey} = \frac{10}{290.52} = 0.0344,$$

$$K_{bc,\,x} = \frac{10}{6.47} = 1.545\,\Omega;\ \ K_{bc,\,y} = \frac{10}{28.36} = 0.353\,\Omega,$$

$$K_{bF} = \frac{10}{\Psi_{2x,\,\max}} = \frac{10}{0.9} = 11.11\,\mathrm{s}^{-1},$$

$$K_{bV} = \frac{u_{V,\,ref}}{\omega_{0rat}} = \frac{10}{157} = 0.064\ \mathrm{Wb},$$

where

$$\omega_{0rat} = \frac{\omega_1}{p_{pol}} = \frac{314}{2} = 157\ \frac{\mathrm{rad}}{\mathrm{s}}.$$

Calculation of parameters for the transfer functions of regulators has been performed.

1. Regulator of current in the axis *x*:

$$\mathrm{W}_{\mathrm{R},\,cx}(\mathrm{s}) = \frac{R_1(\mathrm{s}T_{1x} + 1)}{2\tau K_{bc,\,x}\beta_x \mathrm{s}},$$

where

$$T_{1x} = \frac{L_{1\sigma}}{R_1} = \frac{0.0039}{0.7} = 0.0056\,\mathrm{s},$$

$$\tau = \frac{1}{2f_c} = \frac{1}{2\times 2\times 10^3} = 0.25\times 10^{-3}\,\mathrm{s},$$

$f_c = 2\times 10^3$ Hz is a converter commutating frequency.

Using these data we obtain the transfer function for the *x*-axis current PI-regulator:

$$\mathrm{W}_{\mathrm{R},\,cx}\,(\mathrm{s}) = \frac{0.7\times(1+0.0056\,\mathrm{s})}{2\times 0.25\times 10^{-3}\times 1.545\,\mathrm{s}} = 0.619 + \frac{1}{0.009\,\mathrm{s}}.$$

By analogy with the previous current regulator we write a transfer function for the *y*-axis current PI-regulator:

$$\mathrm{W}_{\mathrm{R},\,cy}\,(\mathrm{s}) = \frac{R_1(\mathrm{s}T_{1y}+1)}{2\tau K_{bc,\,y}\beta_y\,\mathrm{s}},$$

where

$$T_{1y} = \frac{\sigma L_1}{R_1} = \frac{0.068\times 0.143}{0.7} = 0.0139\,\mathrm{s},$$

$$\tau = 0.25\times 10^{-3}\,\mathrm{s};\quad \beta_y = 31;\quad K_{bc,\,y} = 0.353\,\Omega.$$

Putting the values into above equation yields

$$\mathrm{W}_{\mathrm{R},\,cy}\,(\mathrm{s}) = \frac{0.7\times(1+0.00025\,\mathrm{s})}{2\times 0.25\times 10^{-3}\times 31\times 0.353\,\mathrm{s}} = 0.032 + \frac{1}{0.0078\,\mathrm{s}}.$$

2. Rotor flux linkage regulator has the following transfer function

$$\mathrm{W}_{\mathrm{RF}}\,(\mathrm{s}) = \frac{K_{bc,\,x}(\mathrm{s}T_2+1)}{4\tau K_{bF}L_{12}\,\mathrm{s}},$$

where

$$K_{bc,\,x} = 1.545\,\Omega,$$

$$T_2 = \frac{L_2}{R_2'} = \frac{0.145}{0.48} = 0.302\,\mathrm{s};\quad K_{bF} = 11.11\,\mathrm{s}^{-1};\quad L_{12} = 0.139\,\mathrm{H};\quad \tau = 0.25\times 10^{-3}\,\mathrm{s}.$$

At these values a transfer function of the PI-flux linkage regulator takes the form:

$$\mathrm{W}_{\mathrm{RF}}\,(\mathrm{s}) = \frac{1.545\times(1+0.302\,\mathrm{s})}{4\times 0.25\times 10^{-3}\times 11.11\times 0.139\,\mathrm{s}} = 0.302 + \frac{1}{0.998\,\mathrm{s}}.$$

3. For the rotor angular velocity regulator we use a transfer function as follows:

$$\mathrm{W}_{\mathrm{RV}}\,(\mathrm{s}) = \frac{1+8\tau\,\mathrm{s}}{8\tau\,\mathrm{s}}\cdot\frac{JK_{bc,\,y}}{4\tau K_M K_{bV}\Psi_{2m,\,ref}},$$

where

$$J = K_J \cdot J_m = 4 \times 0.028 = 0.112 \text{ kg} \cdot \text{m}^2,$$

$$K_M = \frac{3}{2} p_{pol} K_r = 1.5 \times 2 \times 0.96 = 2.88 ,$$

$$K_{bc,y} = 0.353\,\Omega; \quad \tau = 0.25 \times 10^{-3} \text{ s}; \quad \Psi_{2m,ref} = 0.9 \text{ Wb} .$$

With these data we can obtain a final form of the transfer function for the angular velocity regulator

$$\text{W}_{\text{RV}}(\text{s}) = 238.3 + \frac{1}{8.39 \times 10^{-6} \text{ s}} \approx 238.3 .$$

The calculated values and obtained transfer functions have been used in the Matlab simulation model (Fig. 4) constructed according to the generalized structure of the induction motor vector control system presented in Fig. 3.

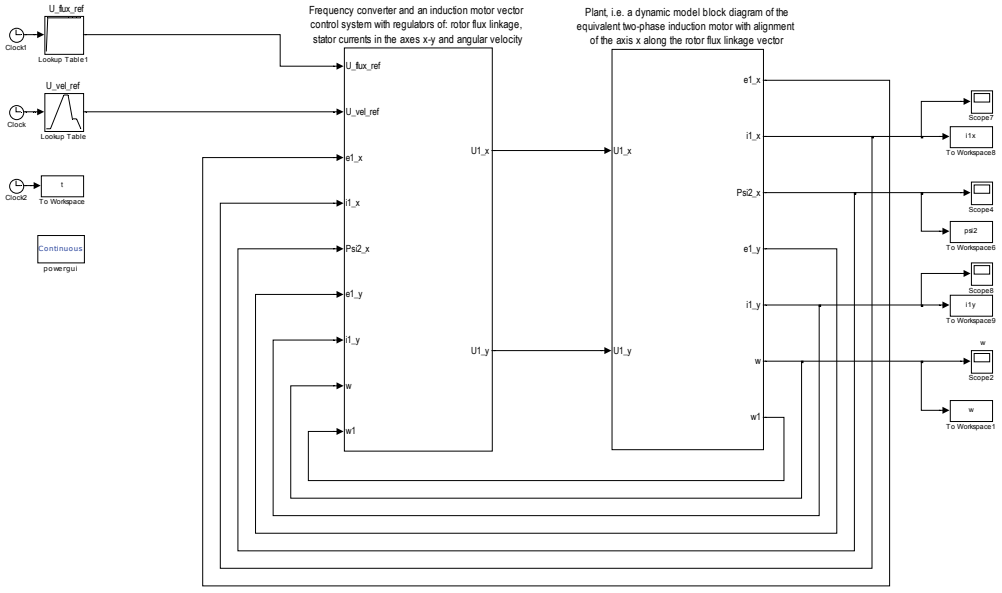

Fig. 4. Simulation model of the induction motor vector control system with alignment of the axis *x* along the rotor flux linkage vector

Simulation results for the induction motor 4A132S4У3 are presented in Fig. 5 and Fig.6. Simulation has been performed under the following drive load and inertia conditions:

$$M_s = M_{rat} = 49 \text{ N} \cdot \text{m}; \quad J = K_J \cdot J_m = 4 \times 0.028 = 0.112 \text{ kg} \cdot \text{m}^2,$$

where

$K_J = 4$ – factor of electrical drive inertia.

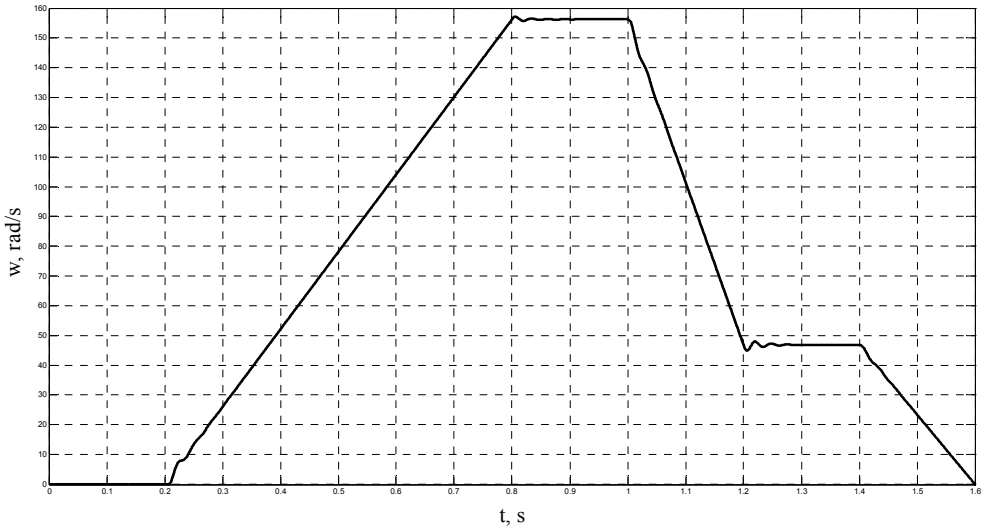

Fig. 5. Rotor angular velocity of the induction motor 4A132S4У3 during vector control with alignment of the axis *x* along the rotor flux linkage vector

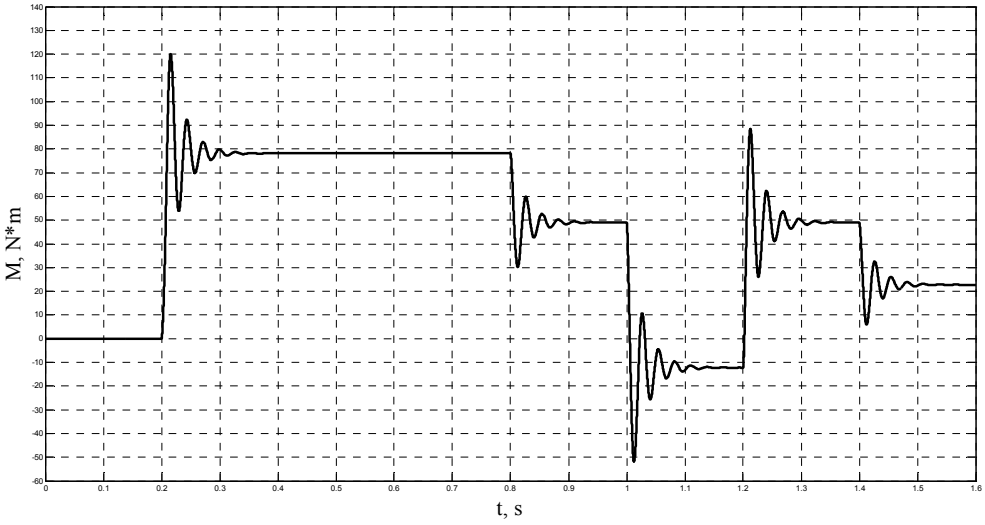

Fig. 6. Electromagnetic torque of the induction motor 4A132S4У3 during vector control with alignment of the axis *x* along the rotor flux linkage vector

4. CONCLUSIONS

1. A technique for investigation of induction motor electric drive dynamics during the operation at the direct vector control with alignment of the axis x along the rotor flux linkage vector has been presented. It includes the faithful representation of dynamic model block diagrams in correspondence with the modern vector control realization along with the revision of analytical expressions for regulator parameter determination.
2. A generalized structure for induction motor vector control with alignment of the axis x along the rotor flux linkage vector has been proposed.
3. Matlab simulation model of the induction motor vector control system with alignment of the axis x along the rotor flux linkage vector build according to the proposed generalized structure has been introduced.
4. Simulation results verify the faithfulness of recommended technique.

REFERENCES

[1] FIRAGO B.I., PAWLACZYK L.B., *Reguliruemye elektroprivody peremennogo toka*, Technoperspektiva, Minsk 2006, 363 s.

[2] FIRAGO B.I., PAWLACZYK L.B., *Teorija elektroprivoda*, 2-e izd., Technoperspektiva, Minsk 2007, 585 s.

[3] VAS P., *Sensorless vector control and direct torque control*, Oxford University Press, Oxford 1998, 728 p.

[4] KOZIARUK A.E., RUDAKOV B.B., *Sovremennoe i perspektivnoe algoritmicheskoe obespechenie chastotno-reguliruemykh elektroprivodov*, Sankt-Peterburgskaya elektrotekhnicheskaya kompaniya, 2004, 127 s.

[5] ANHIMIUK V.L., OPEIKO O.F., MIHEEV N.N., *Teoriya avtomaticheskogo upravleniya*, Dizajn PRO, Minsk 2002, 352 s.

[6] SHREINER R.T., *Matematicheskoe modelirovanie peremennogo toka s poluprovodnikovymi preobrazovatelami chastoty*, URO RAN, Ekateringburg 2000, 654 s.

[7] TRZYNADLOWSKI A.M., *Control of induction motors*, Academic Press, N.Y., London et al., 2001, 228 p.